Proteome Profile Changes During Poly-hydroxybutyrate Intracellular Mobilization in Gram Positive *Bacillus cereus* tsu1

HUI LI
Tennessee State University
Joshua O'Hair
Tennessee State University
Santosh Thapa
Tennessee State University
Sarabjit Bhatti
Tennessee State University
Suping Zhou (zsuping@tnstate.edu)
Tennessee State University
Yong Yang
USDA-ARS
Tara Fish
USDA-ARS
Theodore W. Thannhauser
USDA-ARS

Research article

Keywords: Bacillus cereus, Quantitative proteomics, Poly-hydroxybutyrate, Sporulation, Fermentative growth

Posted Date: April 29th, 2020

DOI: https://doi.org/10.21203/rs.2.15633/v3

Version of Record: A version of this preprint was published at BMC Microbiology on May 19th, 2020. See the published version at https://doi.org/10.1186/s12866-020-01815-6.

Abstract

Background Bacillus cereus is a bacterial species which grows efficiently on a wide range of carbon sources and accumulates biopolymer poly-hydroxybutyrate (PHB) up to 80% cell dry weight. PHB is an aliphatic polymer produced and stored intracellularly as a reservoir of carbon and energy, its mobilization is a key biological process for sporulation in Bacillus spp. Previously, a B. cereus tsu1 was isolated and cultured on rapeseed cake substrate (RCS), with maximum of PHB accumulation reached within 12 h, and depleted after 48 h. Fore-spore and spore structure were observed after 24 h culture.

Results Quantitative proteomic analysis of B. cereus tsu1 identified 2,952 quantifiable proteins, and 244 significantly changed proteins (SCPs) in the 24h-12h pair of samples, and 325 SCPs in the 48h-12h pair of samples. Based on gene ontology classification analysis, biological processes enriched only in the 24h:12h SCPs include purine nucleotide metabolism, protein folding, metal ion homeostasis, response to stress, carboxylic acid catabolism, and cellular amino acid catabolism. The 48h:12h SCPs were enriched into processes including carbohydrate metabolism, protein metabolism, oxidative phosphorylation, and formation of translation ternary structure. A key enzyme for PHB metabolism, poly(R)-hydroxyalkanoic acid synthase (PhaC, KGT44865) accumulated significantly higher in 12h-culture. Sporulation related proteins SigF and SpoEII were significantly higher in 24h-samples. Enzymes for nitrate respiration and fermentation had more accumulation in 48h-culture.

Conclusions Changes in proteome of B. cereus tsu1 during PHB intracellular mobilization were characterized in this study. The key enzyme PhaC for PHB synthesis increased significantly after 12h-culture which supports the highest PHB accumulation at this time point. The protein abundance level of SpoIIE and SigF also increased, correlating with sporulation in 24h-culture. Enzymes for nitrate respiration and fermentation were significantly induced in 48h-culture which indicates the depletion of oxygen at this stage and carbon flow towards fermentative growth. Results from this study provide insights into proteome profile changes during PHB accumulation and reuse, which can be applied to achieve a higher PHB yield and to improve bacterial growth performance and stress resistance.

Background

Bacillus cereus is a gram-positive, facultative anaerobic bacterium that is widely found in soil and other environments. This species of bacteria can grow efficiently by assimilating a wide range of carbon sources including glucose, sucrose, glycerol, oil fat, etc. [1]. It was reported that *B. cereus* can produce intracellular poly-hydroxyalkanoates (PHAs), which can account for up to 80% cell dry weight [2]. PHAs are a class of aliphatic polyesters produced by a large number of bacteria as a reservoir of carbon and energy [3]. Poly-3-hydroxybutyrate (PHB) is the first and most well characterized member in the PHA family discovered in 1925, since then more than 100 polymer structures have been identified in this family with different physical properties [4]. The PHA-derived plastics has become a promising replacement for petroleum-based plastics [5], since it is biodegradable, biocompatible, water insoluble, oxygen permeable and high-temperature resistant. However, the high production cost of PHAs bioplastics remains a major limitation for its commercialization and industrialization [6].

PHA polymers are accumulated and stored as intracellular granules under excess carbon supply, and then mobilized during carbon-limited conditions. Bacterial PHAs synthesis can utilize substrates derived from metabolic pathways such as acetyl-CoA (from glycolysis), enoyl-CoA (from fatty acid β-oxidation) and (R)-3-hydroxy-acyl-ACP (from fatty acid de novo synthesis) [7, 8]. The most prevalent PHB biosynthesis pathway starts with acetyl-CoA and goes through condensation, reduction and polymerization catalyzed by acetyl-CoA acetyltransferase (PhaA), acetoacetyl-CoA reductase (PhaB), PHA synthase (PhaC) respectively for the final PHB production. In another common pathway, enoyl-CoA from fatty acid β-oxidation is first oxidized to (R)-3-hydroxyacyl-CoA by (R)-specific enoyl-CoA hydratase (PhaJ)

before polymerized into PHB polymer by PhaC [9]. The genes encoding for PHB biosynthesis enzymes are often co-localized and organized in an operon. For PHB degradation, the polymer is first depolymerized into its monomer by PHB depolymerase (PhaZ). The elucidation of the PHB reuse mechanism is still in progress. Previous research was able to detect (S)-3-hydroxybutyryl CoA, crotonyl-CoA and acetyl-CoA as PHB degradation intermediates, which links PHB mobilization with other primary and secondary metabolic pathways like glycolysis, β-oxidation, and TCA cycle [10].

In *Bacillus* spp., another key feature is the sporulation process which produces dormant endospores under nutritional stresses [11]. Even though, a variety of self-rescue mechanisms are triggered by starvation, such as the activation of chemotaxis proteins, secretion of hydrolytic enzymes to recycle extracellular energy, sporulation is considered to be the ultimate response [12]. In response to the nutrient depletion as a signal for endospore formation, PHB degradation occurs. In culture, PHB reaches the highest level of accumulation before the formation of fore-spore structure and starts degrading during endospore maturation [13]. More evidences of PHB being mobilized for sporulation came from a study showing that the deficiency in PHB production was associated with reduced spore formation, and the supplementation of exogenous fatty acids was able to recover this sporulation process [14].

When encountering anoxic conditions, many *Bacillus* spp. are capable of using nitrate as electron acceptor, where the various substrate dehydrogenases transfer electrons to the acceptor reductases (nitrate and nitrite reductases). In these *Bacillus* spp., nitrate reduction is always coupled with the fermentative growth, during which ATP is produced by the conversion of pyruvate and acetyl-CoA to a range of fermentative end-products (lactate, acetate, ethanol) [15, 16, 17]. Dissolved oxygen (DO) level is an important factor in PHB production using *Bacillus* spp. A higher PHB yield can be achieved by reducing DO from 40% to 20%, whereas severe PHB degradation was observed when DO further dropped down to 5-10% [18]. Consequently, DO level in culture can determine either the shift of acetyl-CoA towards PHB synthesis or the degradation of stored PHB to feed into other metabolic pathways.

Previously, our lab reported isolation of *B. cereus* tsu1, the genome was predicted to have 5,763 proteins (NCBI accession no. JPYN01; https://www.ncbi.nlm.nih.gov/Traces/wgs/JPYN01?display=proteins&page=1) [19]. In this study, *B. cereus* tsu1 was cultured on rapeseed cake substrate (RCS) without additional supplements as described before [20]. When examined under microscope, the maximum of PHB accumulation was reached within 12 h (before stationary phase) and it was nearly depleted in 48 h (when mature endospores were released). A quantitative proteomic analysis during this process was performed to identify the proteomic profile changes of *B. cereus* tsu1 for a better understanding of PHB mobilization mechanisms and to discover strategies in improving bacterial growth performance to achieve a higher PHB yield.

Results

Growth Phases and PHB Intracellular Mobilization of *B. cereus* tsu1

Bacillus cereus tsu1 was cultured using RCS medium and cells were stained with Sudan black to observe PHB accumulation status (Fig. 1). In 6h-culture, PHB granules were observable but smaller in size. In 9h-culture, the granules aggregated and formed clusters, and reached the highest accumulation before 12 h. Bacterial cells were collected at 12 h, 24 h, 48 h and stored at -20 °C for protein extraction. The reasons for selecting these three time points were 1) bacterial cells in 12h-culture were loaded with PHB when examined using the Sudan black staining method; 2) in 24h-culture, most cells were still filled with PHB, but some cells were sporulating with fore-spore, and spore structure visible under the microscope; 3) significant degradation of PHB was observed in 48h-culture, and even though some mature endospores were released, most cells were still in vegetative state.

Quantitative Proteomic Profile and Identification of Significantly Changed Proteins

SDS phenol based method was used for proteins extraction from bacterial cells cultured in RCS medium for 12, 24 and 48 h. Three biological replicates were included for each time point. After trypsin digestion, samples were labeled with nine tags from a 10-plex tandem mass tags (TMT) kit. The nano-LC-MS/MS identified 3,215 proteins, from where 2,952 proteins were quantified each with two or more unique peptides (Additional file 3: Table S3). The $\log_2$-transformed abundance of all constituent peptides were subjected to a t-test followed by false discovery rate (FDR) correction analysis. A protein with ≥ 1.5 standard deviations from normal distribution curve of each quantified protein and a FDR adjusted p-value ≤ 0.05 was regarded as being significantly changed proteins (SCPs) for each pair of sampling time-points (24h/12h, or 48h/12h). Protein fold changes were obtained from anti-log conversion of $\log_2$ ratios. When comparing 24h- and 12h-samples, there were 244 significantly changed proteins (SCPs) which passed the thresholds [FDR < 0.05, and fold changes (24h/12h) < 0.76 or > 1.31], including 56 up-regulated and 188 down-regulated proteins; in 48h-12h pair of samples, 325 proteins passed the thresholds [FDR < 0.05, and fold changes (48h/12h) < 0.67 or > 1.50], with 145 proteins up-regulated and 180 down-regulated proteins (Fig. 2A, Additional file 1: Table S1-1). Results of t-test and FDR analyses using SAS were listed in the Additional file 2: Table S2-1, Table S2-2.

The identified SCPs were analyzed for functional classification using the PANTHER classification system (v.14.1). The biological processes enriched only in 24h:12h up-regulated SCPs include purine nucleotide metabolism, protein folding, metal ion homeostasis, response to stress; the 24h down-regulated SCPs are classified into processes of carboxylic acid catabolism, cellular amino acid catabolism, peptidoglycan biosynthetic process, RNA process. The 48h:12h SCPs were enriched into biological processes including carbohydrate metabolism, protein metabolism, oxidative phosphorylation, formation of translation ternary structure (Fig. 2B).

Enzymes for PHB Biosynthesis and Intracellular Degradation

The maximum of PHB accumulation in *B. cereus* tsu1 was observed within 12 h. According to a previous study [20], the *B. cereus* tsu1 was annotated with genes in three different pathways for PHB polymerization (Fig. 3). The primary pathway starts with acetyl-CoA, uses enzymes encoded by a *pha* locus which consists of *phaR-phaB-phaC* operon and *phaP-phaQ-phaJ* operon in the opposite direction. The second pathway is using intermediates of fatty acid β-oxidation and catalyzed by acyl-CoA dehydrogenase (AcdA_1 and AcdA_2) and 3-hydroxybutyryl-CoA dehydratase/ enoyl-CoA hydratase (PhaJ). The third pathway involves succinyl-CoA from TCA cycle to produce PHB [21]. And this pathway is catalyzed by SSA dehydrogenase (GabD, KGT45610), 4-hydroxybutyrate dehydrogenase (GabT, KGT45608), and succinyl-CoA-coenzyme A transferase enzyme (ScoT) [7]. STRING database (version 10.5) of *B. cereus* was used for protein-protein interaction network construction of all enzymes in the three PHB synthesis pathways (Fig. 3). In the 48h-sample, PHB was observed to have undergone significant degradation. For PHB degradation, the enzyme 3-oxoadipate enol-lactonase which previously confirmed with PHB intracellular degradation activity in *B. thuringiensis* ATCC35646 [22] was annotated on the *B. cereus* tsu1 genome, and this protein was quantified in this study.

Enzymes for PHB biosynthesis and intracellular degradation and their abundance were compared among the three time-point samples (Fig. 3). Poly(R)-hydroxyalkanoic acid synthase (PhaC, KGT44865) had the highest abundance level at early stage of bacterial growth, while the synthase subunit PhaR (KGT44863) displayed an opposite change. PhaR protein was reported as a global regulation factor, with an impact on PHB biosynthesis [23, 24]. Both 3-oxoacyl-ACP synthase (PhaB, KGT44864) and phasin protein (PhaP, KGT44861) accumulated to the highest abundance level at 48h. PhaQ (KGT44862), which previously identified as a new class of PHB synthesis transcription regulator, was not identified in the proteome analysis. Both AcdA_2 (KGT41138) and PhaJ (KGT44860) involved in PHB biosynthesis using fatty acid β-oxidation intermediate had a higher abundance level at 12 h [25]. Additionally, a majority of enzymes converting glutamate and GABA to PHB were observed with a higher abundance level at 12 h. ScoT (KGT44257) is an

enzyme associated with both PHB synthesis and consumption; its abundance reached the highest level in 48h-sample. Despite of significant PHB degradation observed at 48 h, the abundance of 3-oxoadipate enol-lactonase (KGT42842) for PHB depolymerization was at highest level at 12 h and slightly reduced over time.

PHB Mobilization and Related Metabolic Pathways

In *Bacillus* spp., PHB formation and mobilization are important metabolic processes interacting with other major pathways. As shown in Fig. 4A, PHB biosynthesis starts with acetyl-CoA, which is a molecule that participates in several essential biochemical reactions including glycolysis, lipid and protein metabolism, TCA. PHB mobilization and recycling provide carbon and energy resource for other metabolic pathways such as pyruvate fermentation and butanoate metabolism [26].

In this study, most enzymes in Embden-Meyerhof-Parnas (EMP) pathway, pentose phosphate (PP) pathway, and TCA cycle did not show significant changes among the three time points (Additional file 1: Table S1-2). In EMP, glucose-6-phosphate isomerase (KGT41362) was significantly down-regulated at 0.7 and 0.58 fold in 24h- and 48h-samples. In PP, 6-phosphogluconate dehydrogenase (KGT42918) was down-regulated by 0.66 fold at 48 h. In glyoxylate shunt bypass of TCA, malate synthase (KGT44986), isocitrate lyase (KGT44987) was down-regulated at 0.61 and 0.66 fold respectively at 48 h.

Butanoyl-CoA converted from acetyl-CoA is another major carbon metabolic product. Using this pathway, bacteria can produce butanoate when grown at neutral pH on glucose [27]. The first step in this pathway is identical with PHB biosynthesis. Afterward, acetoacetyl-CoA is converted to (S)-3-hydroxybutanoyl-CoA by 3-hydroxybutyryl-CoA dehydrogenase (KGT41139). The final two-step conversion of butanoyl-CoA to butanoate provides energy source for cells, as ATP is generated. This two-step conversion process is catalyzed by phosphate butyryltransferase (KGT41693) and butyrate kinase (KGT41691). Phosphate butyryltransferase was up-regulated at 1.86 fold at 48 h, and butyrate kinase had a higher abundance at 48 h compared to the other two time points (Fig. 4B, Table 1).

Bacillus spp. can grow by substrate-level phosphorylation/ fermentation under anoxic condition [28]. In *B. cereus* tsu1, formate acetyltransferase (KGT45740) and pyruvate formate lyase-activating protein (KGT45741), which catalyze the reversible conversion of pyruvate into acetyl-CoA using radical non-redox mechanism [29, 30], were up-regulated at 2.11 and 2.2 fold in 48h-culture (Fig. 4B, Table 1). Lactate dehydrogenase (KGT41354) catalyzing the interconversion of pyruvate to lactate was up-regulated at 1.81 fold; lactate utilization protein C (KGT44853), L-lactate dehydrogenase complex protein LldF (KGT44852) and formate dehydrogenase (KGT45530) were up-regulated at 1.84, 1.51 and 1.5 fold respectively in the same culture. For alcohol fermentation, acetyl-CoA is first converted to acetaldehyde by acetaldehyde dehydrogenase (KGT41893), and then to alcohol by ethanol-active dehydrogenase (KGT44011), the latter protein was up-regulated at 1.68 fold. The acetyl-CoA hydrolase (KGT44257) catalyzing the reaction producing acetate from acetyl-CoA also had the highest abundance in 48h-sample.

Acetoin or 3-hydroxybutanoate is another form of carbon and energy storage produced and excreted by bacteria when the pyruvate level is high [31, 32]. It can be used to provide energy for other metabolic pathways at stationary phase [33]. In *B. cereus* tsu1, acetolactate synthase catalytic subunit (KGT44244) and regulatory subunit (KGT44245), acetolactate synthase (KGT44547) and catalytic subunit (KGT44546), acetolactate synthase (KGT45211) were observed with higher abundance level in 12h-culture (Fig. 4B, Additional file 1: Table S1-3). Acetolactate decarboxylase (KGT45212) was not identified in this proteomics analysis. The *acu* operon comprising of acetoin-reuptake enzymes-acetoin dehydrogenase (KGT42181), acetoin utilization protein (KGT42182), histone deacetylase (KGT42183) were not observed with significant changes in abundance. Whereas enzymes in the *aco* operon converting acetoin into acetaldehyde and acetyl-CoA were all up-regulated at 48 h (Table 1), which include dihydrolipoamide dehydrogenase

(KGT43462, 1.72 fold), and acetoin dehydrogenase E1β component (KGT43464, 1.59 fold), acetoin dehydrogenase E1α component (KGT43465, 2.59 fold). R,R-butanediol dehydrogenase (KGT45433) catalyzing the reversible oxidation of 2,3-butanediol to acetoin and the practically irreversible reduction of diacetyl to acetoin was up-regulated at 1.64 fold in 48h-culture [34].

Sporulation and Stress-induced Enzymes

In batch-culture process, bacteria are facing constant stresses such as nutrient depletion and suboptimal pH levels. For gram-positive bacteria like *Bacillus* spp., self-rescue mechanisms under nutrient limitation and environmental stress include induction of chemotaxis protein [35], production of antibiotics [36], secretion of hydrolytic enzymes [37], and finally sporulation. In 24h-sample, pre-spore and spore structures were observed; in 48h-sample, mature endospores were released, meanwhile significant PHB degradation occurred.

In the quantitative proteomic analysis of *B. cereus* tsu1, stress related proteins were identified with significant changes (Fig. 5A, Table 1). Glyoxalase/ lactoylglutathione lyase (KGT43173, KGT42737, KGT42638, KGT44383) [38], chemotaxis protein (KGT45443, KGT41216) [39], activator of Hsp90 ATPase (KGT43768) were significantly higher at 12 h (late exponential phase) compared to 24 h (stationary phase). Molecular chaperone Hsp20 (KGT44005), chaperonin (KGT45779) [7], copper resistance protein CopZ (KGT42404), and RNA-binding protein Hfq (KGT42386) [40] were significantly higher at 24 h. Flagellar hook protein FlgL (KGT44525), flagellin (KGT44484), molecular chaperone DnaJ (KGT45678), disulfide bond formation protein DsbD (KGT45484), anti-terminator HutP (KGT42538) [41], general stress protein (KGT41365), PhoP family transcriptional regulator (KGT42051) [42], sigma-54 modulation protein (KGT40985) and stress protein (KGT43053) had the highest abundance level in 48h-culture.

Thirty-eight proteins related to sporulation were identified with significant change over time (Fig. 5A, Additional file 1: Table S1-4). As the proteins interaction network displayed in Fig. 5B, chemotaxis protein CheY/Spo0A (KGT41699), sporulation sigma factor SigF (KGT41601), anti-sigma F factor (SpoIIAB, KGT41602); anti-sigma F factor antagonist (SpoIIAA, KGT41603), stage II sporulation protein E (SpoII E, KGT45993) are key enzymes involved in sporulation [43, 44]. SigF is the essential enzyme for *Bacillus* spp. sporulation induction. Anti-sigma F factor is the antagonist of SigF, whose activity can be diminished by SpoII E under the regulation of Spo0A [45]. From our results, SigF and SpoII E were up-regulated at 1.43 fold and 1.5 fold, whereas, anti-sigma F factor was down-regulated at 0.65 fold in 24h-culture. The transition state regulator Abh (KGT44175) acts as a transcriptional regulator during the transition state from vegetative growth to stationary phase and sporulation [46], this protein was up-regulated at 1.75 fold and 2.75 fold in 24h- and 48h-cutlures, respectively.

Aerobic Respiration and Anaerobic Respiration

In aerobic bacteria, oxidative phosphorylation is the major metabolic pathway using carbohydrate oxidation to generate ATP. Most ATP molecules are synthesized by five membrane-bound enzyme complexes (electron transport chain system), which include complex I-NADH: ubiquinone oxidoreductase/ NADH dehydrogenase [47], complex II-succinate-Q oxidoreductase/ succinate dehydrogenase [48], complex III-menaquinol-cytochrome c oxidoreductase, complex IV-quinol/cytochrome c oxidase, and complex V-F0F1-ATPase (Additional file 1: Table S1-5) [43, 49]. Most atp operon proteins had higher abundance at early stage (12 h), and ATP synthase F0 subunits B (KGT41105) was significantly higher in 12h-sample compared to the other two time points (Table 1). In 48h-culture, complex III menaquinol-cytochrome C reductase (KGT44670), and complex IV–quinol oxidase subunit 2 (KGT45463, QoxA), cytochrome D ubiquinol oxidase subunit I (KGT42309, CydA) were significantly up-regulated at 1.77 fold, 1.57 fold, 2.33 fold, respectively.

For *Bacillus* spp., the final electron acceptors can also be nitrate, nitrite, nitrous oxide other than O_2 when respiration happens under anaerobic condition [50, 51]. In our quantitative proteomics analysis, nitrate reductase NarG, NarH, NarJ, (KGT44113, 44114, 44115) were significantly up-regulated at 2.47, 1.92, 2.75 fold; nitrite reductase NirD, NirB (KGT44130, 44131) were up-regulated at 1.92, 2.48 fold in 48h-culture (Table 1). These results indicate that, at this time point, the cellular metabolism pathways were changing towards nitrate respiration and fermentation.

Discussion

In this experiment, growth performance and PHB intracellular mobilization of *B. cereus* tsu1 were examined when rapeseed cake substrate (RCS) was used as the sole nutrients for bacterial culture. In batch culture of *B. cereus* tsu1 in RCS, the maximum PHB was observed within 12 h. Significant PHB degradation occurred as well as release of mature endospores in the 48h-culture. The bacterial growth performance in RCS was comparable with cultural media such as LB and minimal salt medium M9 supplemented with glucose, while the PHB accumulation in RCS was earlier (data not shown). The quantitative proteomic analysis of *B. cereus* tsu1 used a holistic approach to investigate the entire proteome expressed in bacterial cells at different cell growth and PHB mobilization stages. Totally 3,215 proteins were identified, out of which 2,952 proteins were quantified in all three time points. Based on PANTHER gene ontology classification, the biological processes enriched with the 24h:12h up-regulated SCPs are more related with stress and cell homeostasis, while the 24h:12h down-regulated SCPs are associated with cellular catabolic processes. In the 48h-12h pair of sample, SCPs were more enriched into carbohydrate/protein metabolism, respiration and energy derivation.

Quantitative proteomics analysis was performed by comparing difference in protein abundance level between 24h- and 12h-samples to determine enzymes related with PHB biosynthesis, cellular stress and sporulation; and by comparing between 48h- and 12h-samples for detection of enzymes associated with PHB degradation and other metabolic pathways.

Enzymes for PHB biosynthesis and intracellular degradation were quantified in this proteomic analysis, even though, a majority of enzymes were not observed to have significantly abundance changes across the three cultures at 12, 24 and 48 h. PhaC is the key enzyme in PHB polymerization [52] and a significantly higher abundance of PhaC was observed in 12h-culture. Accordingly, a shorter interval of sampling strategy should be applied in future studies of the related enzymes. PhaJ is the key enzyme to provide (R)-3HB-CoA monomer for PHB synthesis in the second pathway. Both PhaJ, and enzymes using succinyl-CoA to produce PHB were identified in 12h-culture, which is an evidence that the bacterium is using all three pathways for PHB accumulation [53, 54]. Additionally, the 3-oxoadipate enol-lactonase catalyzing PHB intracellular degradation showed the highest level in the same 12h-culture. Taken together, these results indicate that the PHB synthesis and utilization processes occurred simultaneously in these cells. In another research using mutant *B. thuringiensis* BMB171 as a model organism, PHB degradation remained active even when the gene encoding for 3-oxoadipate enol-lactonase was deleted, which implies that other enzymes are responsible for PHB degradation as well [55]. The enzyme 3-oxoadipate enol-lactonase of *B. thuringiensis* contains a lipase box-like sequence (G-W-S102-M-G), and the serine (102) site was proved to be important for the PHB-hydrolyzing activity [22]. Protein BLAST of 3-oxoadipate enol-lactonase (KGT42842) on NCBI classified it as an alpha/beta hydrolase superfamily protein. To look for other potential proteins contributing to PHB degradation, alpha/beta hydrolase superfamily proteins on annotated genome of *B. cereus* tsu1 were downloaded, and multiple sequence alignment were performed to compare sequence homology and to detect putative lipase box-like sequence [56]. As shown in Additional File 4: Fig. S1, alpha/beta hydrolase family proteins KGT43118, KGT41369, KGT41644, KGT42270 were all detected with G-X-S-X-G lipase-box sequence. Bacteria experiencing incomplete PHB mobilization were observed with deficient sporulation and lower stress tolerance. Therefore, enzymes catalyzing PHB degradation play a crucial role in bacterial

survival under unfavorable conditions. The potential PHB degradation enzymes can become targets in future study to increase PHB yield and improve bacterial growth performance.

Spo0A plays a significant role in bacterial sporulation by regulating the activation of SpoII E. SpoIIE-RodZ complex was reported coordinating in asymmetric septum formation and SigF activation in *B. subtilis* [57]. Anti-sigma F can bind on SigF and block its ability to form an RNA polymerase holoenzyme (E-sigma F). The function of anti-sigma F can be eliminated by SpoII E [58, 59]. In this study, SpoII E and SigF were observed with significant up-regulation, while anti-sigma F was significantly down-regulated at 24 h. Nevertheless, the transcription factor Spo0A did not have significant abundance change across the culture period. As the concurrence of sporulation and PHB degradation was always observed in spore forming bacteria, previous studies suggested that suppression of sporulation can be used as a strategy to improve PHB yield. But in the experiment, the mutant *B. thuringiensis* with deletion of *spo0A* was found severely impaired in PHB accumulation [45]. It was concluded that the Spo0A transcription factor is required for a global regulation of PHB biosynthesis, sporulation and other cell cycles. As the protein abundance of both SpoII E and SigF was significantly increased during forespore formation, these two proteins can be promising targets in reducing sporulation and improving PHB biosynthesis.

At 48 h, enzymes for nitrate respiration were highly induced, which is an indicator of oxygen limitation during batch-culture [60]. At this period of time, enzymes for pyruvate fermentation into formate, lactate, ethanol were significantly induced; the abundance of phosphate butyryltransferase (KGT41693) and butyrate kinase (KGT41691) for butanoate biosynthesis reached the highest level [61]; expression of proteins for the acetoin and butanediol metabolism were also highly induced. These pathways utilize the same carbon sources as PHB biosynthesis, which might need to consume products from PHB degradation [32]. These results concurred with the significant degradation of PHB in the cells at 48 h.

Conclusions

Proteome profile changes during PHB intracellular mobilization in *Bacillus cereus* tsu1 was identified in this study. Our results revealed: 1) The key enzyme PhaC for PHB synthesis and 3-oxoadipate enol-lactonase for PHB degradation were detected in all samples and both reached a higher abundance in 12h-culture implying the concurrence of PHB synthesis and utilization at this time point; 2) the protein abundance level of SpoIIE and SigF was significantly increased to induce asymmetric septum formation and sporulation, these two can be promising target genes for delaying sporulation and thus increasing PHB accumulation; 3) when oxygen became limited, enzymes for nitrate respiration and fermentation were induced to compete for the carbon resource with PHB biosynthesis.

PHB production in non-spore forming bacteria can be induced by excess carbon and imbalanced nutrients conditions (depleted nitrogen, phosphorus, and low oxygen); whereas the same condition will lead to sporulation, fermentative growth and PHB consumption in *Bacillus* strains. In this context, results from this study provide insights into the proteome profile changes during PHB accumulation and recycling in *B. cereus* tsu1. The identified proteins (genes) can be targeted for modification to achieve a higher PHB yield and to improve bacterial growth performance and stress resistance in *Bacillus* spp.

Methods

Bacterial culture

In our previous research [19, 20], we have reported the isolation and genome analysis of *B. cereus* tsu1. The genome sequence is available in NCBI database under accession No. JPYN01.

Bacillus cereus tsu1 was cultured in 50-ml tube containing 20 ml rapeseed cake substrate (RCS, 2.5% aqueous extract). A fresh overnight (16 h) single-colony culture in LB broth was used as inoculum (at 1:100 ratio). Bacterial cultures were agitated at 200 rpm and 30 °C. Cells were taken from the culture at 6, 9, 12, 24, 48 h and stained with Sudan Black to observe PHB accumulation under a microscope equipped with 506 color camera and 63X oil lens (Axioimager M2, Zeiss) [62]. Cell samples were collected at 12, 24, and 48 h by centrifugation at 13,000 × g, for 5 min. Triplicate cultures were included for each time point.

Protein sample preparation and TMT labeling

Proteins were extracted from cell pellets using the SDS phenol based protein extraction method [63]. Briefly, frozen bacterial cell pellets were re-suspended in a buffer containing 2% sodium dodecyl sulfate (SDS), 30% sucrose, 5% β-mercaptoethanol (v/w) prepared in 0.1 M Tris-HCl (pH 8.0) and ground using a Retsch Mixer Mill MM 400 (Retsch GmbH, Germany). Cold phenol was added at 1:1 ratio and the samples were incubated at 4 °C for 2 h. The mixture was centrifuged at 13,000 × g 4 °C for 20 min, and protein in the upper phenol phase was precipitated in methanol containing 0.1 M ammonium acetate after overnight incubation at −20 °C. After a serial of washes in methanol followed by acetone, the air-dried protein pellets were solubilized in 100 mM triethylammonium bicarbonate (TEAB) buffer. Protein concentration was determined using a Qubit Protein Assay Kit (Thermo Fisher Scientific, MA) on a Qubit 3.0 Fluorometer (Invitrogen, CA).

For TMT labeling, a100 µg protein sample was processed following the instructions in the TMT10plex™ Isobaric Label Reagent Set (Thermo Fisher Scientific). Protein tryptic digestion was conducted using Sequencing Grade Modified Trypsin (Promega, WI) with incubation at 37 °C for 16 h. The three replicates of bacterial samples grown for 12 h were labeled with tags 126, 128C, 129N; 24 h samples with 127N, 131 and 129C; and 48 h samples with 127C, 130N, 128N [64]. After combining all the labeled samples, SDS and nonionic solvents were removed using Oasis MCX cartridge following the manufacturer's instructions (Waters; MA). Peptides were eluted in 75% acetonitrile (ACN)/10% NH_4OH and dried at reduced pressure using a CentiVac Concentrator (labConco, MO). Prior to reconstitution for analysis by mass spectrometry, the samples were re-suspended in 100 µl deionized water and re-dried.

Nano LC-MS/MS analysis

The high pH reverse phase high performance liquid chromatography (hpRP-HPLC) was carried out using a Dionex UltiMate 3000 HPLC system with the built-in micro fraction collection option in its autosampler and UV detection (Sunnyvale, CA) as reported previously [65]. The TMT 10-plex tagged tryptic peptides were reconstituted in buffer A (20 mM ammonium formate pH 9.5 in water), and loaded onto an XTerra MS C18 column (3.5 µm, 2.1x150 mm) from Waters (Milford, MA). The peptides were eluted using a gradient of 10-45% of buffer B (80% ACN/20% 20mM NH_4FA) in 30 min at a flow rate 200 µL/min. Forty-eight fractions were collected at 1 min intervals and pooled into a total of 12 fractions based on the UV absorbance at 214 nm and with multiple fraction concatenation strategy [66]. All of the fractions were dried and reconstituted in 100 µL of 2% ACN/0.5% FA for Nano LC-MS/MS analysis.

The Nano LC-MS/MS analysis was carried out using an Orbitrap Fusion (Thermo Fisher Scientific) mass spectrometer equipped with nano ion source using high energy collision dissociation (HCD) similar to previous reports [67]. The Orbitrap was coupled with the UltiMate 3000 RSLCnano (Dionex, CA). Each reconstituted fraction (8 µL) was injected onto a PepMap C-18 RP nano trap column (3 µm, 75 µm X 20 mm, Dionex) at 20 µL/min flow rate for on-line desalting. And all fractions were then separated on a PepMap C-18 RP nano column (3 µm, 75µm x 15cm), and eluted with gradient of 5% to 38% acetonitrile (ACN) in 0.1% formic acid at 300 nL/min in 120 min, followed by a 7-min ramping to 95% ACN/0.1% FA and a 7-min holding at 95% ACN/0.1% FA. The column was re-equilibrated with 2% ACN/0.1% FA for 20 min prior to the next run. The Orbitrap Fusion was operated in positive ion mode with nano spray voltage set at 1.6

kV and the source temperature at 275 °C. External calibration for FT, IT and quadrupole mass analyzers was performed. An internal calibration was performed using the background polysiloxane ion signal at m/z 445.120025 as the calibrant. The instrument was operated in data-dependent acquisition (DDA) mode using FT mass analyzer for one survey MS scan for selecting precursor ions, followed by top 3 s data-dependent HCD-MS/MS scans for precursor peptides with 2-7 charged ions above a threshold ion count of 10,000 with normalized collision energy of 37.5%. MS survey scanned at a resolving power of 120,000 (fwhm at m/z 200), for the mass range of m/z 400-1600 with AGC and Max IT settings of 3e5 and 50 ms, respectively. MS/MS scans for the mass range m/z 105-2000 were conducted at a resolving power of 50,000 (fwhm) with AGC, MaxIT settings of 1e5, 120 ms and with a Q isolation window (m/z) at 1.6. Dynamic exclusion parameters were set at 1 with ±10 ppm exclusion mass width within 50s exclusion duration. All data was acquired under Xcalibur 3.0 operation software and Orbitrap Fusion Tune 2.0 (Thermo Fisher Scientific).

Protein identification and quantification

All MS/MS raw spectra were processed and database searched using Sequest HT software within the Proteome Discoverer 2.2 (PD 2.2, Thermo Fisher Scientific). *Bacillus cereus* tsu1 protein database (which was constructed using six-frame translation of the assembled genome sequence) was used to search the spectra (database download link: https://www.ncbi.nlm.nih.gov/protein?linkname=bioproject_protein&from_uid=256220). The search parameters were set as two mis-cleavages for full trypsin with fixed carbamidomethyl of cysteine, fixed 10-plex TMT modifications on lysine and N-terminal amines and variable modifications of methionine oxidation and deamidation on asparagine and glutamine residues. The peptide mass tolerance and fragment mass tolerance values were 10 ppm and 50 mDa, respectively. Identified peptides were filtered for a maximum 1% FDR using the Percolator algorithm in PD 2.2 along with peptide confidence set to high. The TMT10-plex quantification method within PD 2.2 was used to calculate the reporter ratios with a mass tolerance ±10 ppm without applying isotopic correction factors. Only peptide spectra containing all reporter ions were designated as “quantifiable spectra” and used for peptide/protein quantitation.

Significantly changed proteins (SCPs) identification, PANTHER and STRING Analysis

For protein quantification analysis it requires that a protein is reported with two or more unique peptides across all biological samples. The $\log_2$-transformed abundance of all constituent peptides of proteins identified with at least two unique peptides were subjected to a quantification study using t-test (General Linear Model) followed by false discovery rate (FDR) analysis. The $\log_2$ ratios of peptides were fitted to a normal distribution, one and half standard deviations (±1.5 SD, i.e., a 90% confidence level) and a FDR adjusted p-value ≤ 0.05 were used as the cut-off threshold values for significantly changed proteins. SCPs fold changes were obtained from anti-log conversion of $\log_2$ ratios. The statistical analysis was conducted using SAS (version 9.4) [68].

Gene Ontology (GO) functional classification of 24-12h pair, and 48-12h pair SCPs was performed using the PANTHER classification system (v.14.1, http://www.pantherdb.org). The gene IDs of SCPs were submitted to the database to carry out PANTHER Overrepresentation test using the PANTHER GO-Slim Biological Process [69]. Proteins assigned to at least one category could be counted more than once. The STRING database (10.5, https://version-10-5.string-db.org) was used to predict protein-protein interaction networks based on certain active interaction sources including textmining, experiments, database, co-expression, neighborhood, gene fusion, co-occurrence [70]. Protein network analysis was performed by submitting SCPs sequences to the STRING database. Medium confidence (0.400) was applied and disconnected nodes were hidden. Protein clusters were created using the Markov Cluster Algorithm (MCL) inflation parameter (MCL=3). Lines between nodes represent their action effects, while continuous lines representing direct interactions, interrupted lines indicating indirect functional connections. Protein sequences of functionally enriched proteins were subjected to illustrate the possible molecular actions between each other.

Abbreviations

PHB: poly-hydroxybutyrate

RCS: Rapeseed Cake Substrate

B. cereus: *Bacillus cereus*

SigF: Sigma factor F

SpoE II: Stage II sporulation protein E

SCPs: Significantly Changed Proteins

PHAs: Poly-hydroxyalkanoates

DO: Dissolved Oxygen

TMT: Tandem Mass Tags

FDR: False Discovery Rate

EMP: Embden–Meyerhof–Parnas

PP: Pentose Phosphate

TCA: Tricarboxylic Acid Cycle

ATP: Adenosine Triphosphate

BLAST: Basic Local Alignment Search Tool

B. subtilis: *Bacillus subtilis*

B. thuringiensis: *Bacillus thuringiensis*

STRING: Search Tool for the Retrieval of Interacting Genes

MCL: Markov Cluster Algorithm

Declarations

AVAILABILITY OF DATA AND MATERIALS

The mass spectrometry proteomics data were deposited to the ProteomeXchange database (http://proteomexchange.org/) via the PRIDE partner repository with identifier PXD009960 under project title: TMT-quantitative proteomic study of *Bacillus cereus* tsu1. All other data generated or analyzed during this study are included in this manuscript.

DECLARATIONS

Ethics approval and consent to participate

Not applicable.

Consent for publication

Not applicable.

Competing interests

The authors declare that they have no competing interests.

ARS disclaimer: “Mention of trade names or commercial products in this publication is solely for the purpose of providing specific information and does not imply recommendation or endorsement by the U.S. Department of Agriculture. The funders of the project had no role in study design, data collection and interpretation, or the decision to submit the work for publication.

FUNDING

This research was supported by the National Institutes of Food and Agriculture (NIFA), U.S. Department of Agriculture, grant number 2018-38821-27737 for the 1890 Capacity Building Grants Program.

ACKNOWLEDGEMENTS

The authors wish to thank Dr. Sheng Zhang of the Proteomics and Mass Spectrometry Facility at the Cornell University Institute of Biotechnology for expert technical assistance and helpful discussions for the proteomics analysis. We also thank Dr. Jason P. de Koff for kindly providing rapeseed cake materials and Mr. Dwane Adams for professional instructions in using the imaging system.

AUTHOR INFORMATION

Affiliations

Department of Agricultural and Environmental Sciences, College of Agriculture, Tennessee State University, 3500 John Merritt Blvd, Nashville, TN 37209, U.S.

Hui Li, Joshua O’Hair, Santosh Thapa, Sarabjit Bhatti, Suping Zhou

R.W. Holley Center for Agriculture and Health, USDA-ARS, Cornell University, Ithaca, NY 148532, U.S.

Yong Yang, Tara Fish, Theodore W. Thannhauser

Corresponding authors

Correspondence to Suping Zhou

Contributions

HL, ST, SZ designed the study and performed quantitative proteomic experiment; TF, YY performed Mass Spectrometry analysis; HL, JO performed SAS statistical analysis; HL wrote the manuscript; SB, SZ, and TT critically reviewed and edited drafts of the manuscript and gave important suggestions on interpretation of results and discussion. All authors have read and approved the manuscript.

Supplementary Information

Additional file 1:

Table S1-1. Significantly changed proteins identified in pair of 24h:12h and 48h:12h.

Table S1-2. EMP, PP, TCA enzymes and their average abundance in three time-point samples.

Table S1-3. Enzymes in butanoate and pyruvate anaerobic metabolism and the abundance at three different time points.

Table S1-4. Significantly changed proteins related with sporulation.

Table S1-5. Protein abundance of enzymes involved in oxidative phosphorylation and anaerobic/nitrate respiration.

Table S1-6. PHB biosynthesis and intracellular degradation enzymes and their average abundance in three time-point samples.

Additional file 2

Table S2-1. T-test and FDR analysis of 24h-12h pair of samples.

Table S2-2. T-test and FDR analysis of 48h-12h pair of samples.

Additional file 3

Table S3. Proteins identified and their normalized abundances in *Bacillus cereus* tsu1 in 12h-, 24h-, and 48h-culture.

Additional file 4

Figure S1. Multiple sequence alignment of A/B hydrolase superfamily proteins on B. cereus tsu1 genome.

References

1. Zigha A, Rosenfeld E, Schmitt P, Duport C. The Redox Regulator Fnr Is Required for Fermentative Growth and Enterotoxin Synthesis in *Bacillus cereus* F4430 / 73. J Bacteriol. 2007;189:2813-2824. http://doi.org/10.1128/JB.01701-06.
2. Kumar P, Patel SKS., Lee JK, Kalia VC. Extending the limits of *Bacillus* for novel biotechnological applications. Biotechnol Adv. 2013;31(8):1543-1561. doi:10.1016/j.biotechadv.2013.08.007.
3. Łabużek S, Radecka I. Biosynthesis of PHB tercopolymer by *Bacillus cereus* Journal of Applied Microbiology. 2001;90:353-357. https://doi.org/10.1046/j.1365-2672.2001.01253.x.
4. Keshavarz T, Roy I. Polyhydroxyalkanoates: bioplastics with a green agenda. Curr Opin Microbiol. 2010;13:321-326. http://doi.org/10.1016/j.mib.2010.02.006.
5. Park SJ, Lee SY, Lee Y. Biosynthesis of (R)-3-Hydroxyalkanoic Acids by Metabolically Engineered *Escherichia coli*. In: Finkelstein M., McMillan J.D., Davison B.H., Evans B. (eds), Biotechnology for Fuels and Chemicals (The Twenty-Fifth Symposium). Totowa: Humana Press; 2004.
6. Chen G. A microbial polyhydroxyalkanoates (PHA) based bio- and materials industry. Chem Soc Rev. 2009;38(8):2434-2446. http://doi.org/10.1039/b812677c.

7. Wu D, He J, Gong Y, Chen D, Zhu X, Qiu N, Sun M, Li M, Yu Z. Proteomic analysis reveals the strategies of *Bacillus thuringiensis* YBT-1520 for survival under long-term heat stress. Proteomics. 2011;11:2580–2591. http://doi.org/10.1002/pmic.201000392.
8. Antelmann H, Sapolsky R, Miller B, Ferrari E, Chotani G, Weyler W, Gaertner A, Hecker M. Quantitative proteome profiling during the fermentation process of pleiotropic *Bacillus subtilis* Proteomics. 2004;4:2408–2424. http://doi.org/10.1002/pmic.200300752.
9. Mizuno K, Kihara T, Tsuge T, et al. Cloning and heterologous expression of a novel subgroup of class IV polyhydroxyalkanoate synthase genes from the genus *Bacillus*. Biosci Biotechnol Biochem. 2017;8451:1-3. doi:10.1080/09168451.2016.1230006.
10. Uchino K, Saito T, Gebauer B, Jendrossek D. Isolated Poly(3-Hydroxybutyrate) (PHB) Granules Are Complex Bacterial Organelles Catalyzing Formation of PHB from Acetyl Coenzyme A (CoA) and Degradation of PHB. J Bacteriol. 2007;189(22):8250-8256. doi:10.1128/JB.00752-07.
11. Piggot PJ, Hilbert DW. Sporulation of *Bacillus subtilis*. Curr Opin Microbiol. 2004;7:579–586. http://doi.org/10.1016/j.mib.2004.10.001.
12. Cohn R. *Bacillus subtilis* and its relatives: molecular biological and industrial workhorses. Trends Biotechnol. 1992;10:247-256. https://doi.org/10.1016/0167-7799(92)90233-L.
13. Ray S, Kalia VC. Polyhydroxyalkanoate Production and Degradation Patterns in *Bacillus* Indian J Microbiol. 2017;10:247-256. http://doi.org/10.1007/s12088-017-0676-y.
14. Sadykov MR, Ahn J, Widhelm TJ, Eckrich VM, Endres JL, Driks A, Rutkowski GE, Wingerd KL, Bayles KW. Poly(3-hydroxybutyrate) fuels the tricarboxylic acid cycle and de novo lipid biosynthesis during *Bacillus anthracis* Mol Microbiol. 2017;104:793-803. http://doi.org/10.1111/mmi.13665.
15. Chumsakul O, Anantsri DP, Quirke T, Oshima T, Nakamura K, Ishikawa S, Nakano MM. Genome-wide analysis of ResD, NsrR, and Fur binding in *Bacillus subtilis*during anaerobic fermentative growth by *in vivo* J Bacteriol. 2017;199:e00086-17. https://doi.org/10.1128/JB.00086-17.
16. Ye RW, Tao W, Bedzyk L, Young T, Chen M. Global Gene Expression Profiles of *Bacillus subtilis* Grown under Anaerobic Conditions. J Bacteriol. 2000;182:4458–4465. https://doi.org/10.1128/JB.182.16.4458-4465.2000.
17. Clements LD, Streips UN, Miller BS. Differential proteomic analysis of *Bacillus subtilis* nitrate respiration and fermentation in defined medium. Proteomics. 2002;2:1724–1734. https://doi.org/10.1002/1615-9861(200212)2:12<1724::AID-PROT1724>3.0.CO;2-S.
18. Faccin DJL, Rech R, Secchi AR, Cardozo NSM, Ayub MAZ. Influence of oxygen transfer rate on the accumulation of poly(3-hydroxybutyrate) by *Bacillus megaterium*. Process Biochem. 2013;48(3):420-425. doi:10.1016/j.procbio.2013.02.004.
19. Li H, Zhou S, Johnson T, Vercruysse K, Ropelewski AJ, Thannhauser W. Draft Genome Sequence of a New *Bacillus cereus* Strain tsu1. Genome Announcements. 2014;2:e01294-14. http://doi.org/10.1128/genomeA.01294-14.
20. Li H, Zhou S, Johnson T, Vercruysse K, Lizhi O, Ranganathan P, Phambu N, Ropelewski AJ, Thannhauser TW. Genome Structure of *Bacillus cereus* tsu1 and Genes Involved in Cellulose Degradation and Poly-3-Hydroxybutyrate Synthesis, International Journal of Polymer Science. 2017;2017:6192924. https://doi.org/10.1155/2017/6192924.
21. Chen D, Xu D, Li M, He J, Gong Y, Wu D. Proteomic analysis of *Bacillus thuringiensis* Δ *phaC* mutant BMB171 / PHB−1 reveals that the PHB synthetic pathway warrants normal carbon metabolism. J Proteomics. 2012;75:5176-5188. http://doi.org/10.1016/j.jprot.2012.06.002.

22. Tseng C, Chen H, Shaw G. Identification and Characterization of the *Bacillus thuringiensis* phaZ Gene, Encoding New Intracellular Poly-3-Hydroxybutyrate Depolymerase. J Bacteriol. 2006;188:7592–7599. http://doi.org/10.1128/JB.00729-06.
23. Hyakutake M, Saito Y, Tomizawa S, Mizuno K. Polyhydroxyalkanoate (PHA) Synthesis by Class IV PHA Synthases Employing *Ralstonia eutropha* PHB 4 as Host Strain. J Bioscience, Biotechnology, and Biochemistry. 2014;75: 1615-1617. http://doi.org/10.1271/bbb.110229.
24. Quelas JI, Mesa S, Mongiardini EJ, Jendrossek D, Lodeiro AR. Regulation of Polyhydroxybutyrate Synthesis in the Soil Bacterium *Bradyrhizobium diazoefficiens*. Appl Environ Microbiol. 2016;82:4299-4308. http://doi.org/10.1128/AEM.00757-16.
25. Tajima K, Igari T, Nishimura D, Nakamura M, Satoh Y, Munekata M. Isolation and Characterization of *Bacillus sp.* INTO05 accumulating Polyhydroxyalkanoate (PHA) from Gas Field Soil. J Biosci Bioeng. 2003;95:77-81. https://doi.org/10.1016/S1389-1723(03)80152-4.
26. Ireton K, Jint S, Grossman AD, Sonensheintt L. Krebs cycle finction is required for activation of the Spo0A transcription factor in *Bacillus subtilis*. PNAS. 1995;92:2845-2849. https://doi.org/10.1073/pnas.92.7.2845.
27. Bennett GN, Rudolph FB. The central metabolic pathway from acetyl-CoA to butyryl-CoA in *Clostridium acetobutylicum*. FEMS Microbiology Rev. 1995;17:241–249. https://doi.org/10.1111/j.1574-6976.1995.tb00208.x.
28. Nakano MM, Dailly YP, Zuber P, Clark DP. Characterization of Anaerobic Fermentative Growth of *Bacillus subtilis*: Identification of Fermentation End Products and Genes Required for Growth. J Bacteriol. 1997;179:6749–6755. http://doi.org/10.1128/jb.179.21.6749-6755.1997.
29. Marsh ENG. A radical approach to enzyme catalysis. BioEssays. 1995;17:431–441. https://doi.org/10.1002/bies.950170511.
30. Wolfe AJ. The Acetate Switch. Microbiol Mol Biol Rev. 2005;69:12–50. http://doi.org/10.1128/MMBR.69.1.12
31. Speck EL, Freese E. Control of Metabolite Secretion in *Bacillus subtilis*. Journal of General Microbiol. 1973;78:261–275. http://doi.org/1099/00221287-78-2-261.
32. Kominek LA, Halvorson HO. Metabolism of Poly-beta-Hydroxybutyrate and Acetoin in *Bacillus cereus*. J Bacteriol. 1965;90:1251-1259.
33. Yang S, Dunman PM, Projan SJ, Bayles KW. Characterization of the *Staphylococcus aureus* CidR regulon: elucidation of a novel role for acetoin metabolism in cell death and lysis. Molecular Microbiol. 2006;60:458–468. http://doi.org/10.1111/j.1365-2958.2006.05105.x.
34. Zhang X, Bao T, Rao Z, Yang T, Xu Z, Yang S. Two-Stage pH Control Strategy Based on the pH Preference of Acetoin Reductase Regulates Acetoin and 2,3-Butanediol Distribution in *Bacillus subtilis*, Plos one. 2014;9:e91187. http://doi.org/10.1371/journal.pone.0091187.
35. Maurer LM, Yohannes E, Bondurant SS, Radmacher M, Slonczewski JL. pH Regulates Genes for Flagellar Motility, Catabolism, and Oxidative Stress in *Escherichia coli* K-12†. J Bacteriol. 2005;187:304–319. http://doi.org/10.1128/JB.187.1.304.
36. Hibbing ME, Fuqua C, Parsek MR, Peterson SB. Bacterial competition: surviving and thriving in the microbial Jungle. Nat Rev Microbiol. 2010;8:15–25. http://doi.org/10.1038/nrmicro2259.Bacterial
37. Szilagyi M, Miskei M, Karanyi Z, Lenkey B, Pocsi I, Emri T. Transcriptome changes initiated by carbon starvation in *Aspergillus nidulans*. Microbiology. 2013;159:176–190. http://doi.org/10.1099/mic.0.062935-0.
38. Leelakriangsak M, Thi N, Huyen T, Töwe S, van Duy N, Becher D, Hecker M, Antelmann H, Zuber P. Regulation of quinone detoxification by the thiol stress sensing DUF24/MarR-like repressor, YodB in *Bacillus subtilis*. Mol Microbiol. 2008;67:1108–1124. http://doi.org/10.1111/j.1365-2958.2008.06110.x.

39. Schmid R, Graumann P, Schro K. Cold Shock Stress-Induced Proteins in *Bacillus subtilis*. J Bacteriol. 1996;178:4611–4619. http://doi.org/10.1128/jb.178.15.4611-4619.1996.
40. Christiansen JK, Larsen MH, Ingmer H, Søgaard-andersen L, Kallipolitis BH. The RNA-Binding Protein Hfq of *Listeria monocytogenes*: Role in Stress Tolerance and Virulence. J Bacteriol. 2004;186:3355–3362. http://doi.org/10.1128/JB.186.11.3355.
41. Gopinath SCB, Balasundaresan D, Kumarevel T, Misono TS, Mizuno H, Kumar PKR. Insights into anti-termination regulation of the hut operon in *Bacillus subtilis*: importance of the dual RNA-binding surfaces of HutP. Nucleic Acids Res. 2008;36:3463–3473. http://doi.org/10.1093/nar/gkn199.
42. Hulett FM. The signal-transduction network for Pho regulation in *Bacillus subtilis*. Mol Microbiol. 1996;19:933–939. https://doi.org/10.1046/j.1365-2958.1996.421953.x.
43. Wang J, Mei H, Zheng C, Qian H, Cui C, Fu Y,Su J, Liu Z, Yu Z, He J. The Metabolic Regulation of Sporulation and Parasporal Crystal Formation in *Bacillus thuringiensis* Revealed by Transcriptomics and Proteomics. Mol Cell Proteomics. 2013;12:1363–1376. http://doi.org/10.1074/mcp.M112.023986.
44. Higgins D, Dworkin J. Recent progress in *Bacillus subtilis* FEMS Microbiol Rev. 2012;36:131–148. http://doi.org/10.1111/j.1574-6976.2011.00310.x.
45. Chen H, Tsai T, Pan S, Lin J, Tseng C, Shaw G. The master transcription factor Spo0A is required for poly(3-hydroxybutyrate) (PHB) accumulation and expression of genes involved in PHB biosynthesis in *Bacillus thuringiensis*. FEMS Microbiol Lett. 2010;304:74–81. http://doi.org/10.1111/j.1574-6968.2009.01888.x.
46. Strauch MA, Perego M, Burbulys D. The transition state transcription regulator AbrB of *Bacillus subtilis* is autoregulated during vegetative growth. Mol Microbiol. 1989;3:1203-1209. https://doi.org/10.1111/j.1365-2958.1989.tb00270.x.
47. Friedrich T, Weiss H. Modular Evolution of the Respiratory NADH: Ubiquinone Oxidoreductase and the Origin of its Modules. J Theor Biol. 1997;187:529–540. https://doi.org/10.1006/jtbi.1996.0387.
48. Hederstedt L, Rutberg L. Biosynthesis and Membrane Binding of Succinate Dehydrogenase in *Bacillus subtilis*. J Bacteroil. 1980;144:941–951.
49. Hicks DB, Wang Z, Wei Y, Kent R, Guffanti AA, Banciu H, Bechhofer DH, Krulwich TA. A tenth *atp*gene and the conserved *atpI* gene of a *Bacillus atp* operon have a role in Mg2+ uptake. PNAS. 2003;100(18):10213-10218; https://doi.org/10.1073/pnas.1832982100.
50. Morozkina E V, Zvyagilskaya RA. Nitrate Reductases: Structure, Functions, and Effect of Stress Factors. Biochemistry (Moscow). 2007;72:1151–1160. /S0006297907100124.
51. Downey, R. J. Nitrate Reductase and Respiratory Adaptation in *Bacillus stearothermophilus*. J Bacteroil. 1966;91(2):634–641.
52. Tsuge T, Hyakutake M, Mizuno K. Class IV polyhydroxyalkanoate (PHA) synthases and PHA-producing *Bacillus*. Appl Microbiol Biotechnol. 2015;99:6231-6240. http://doi.org/10.1007/s00253-015-6777-9.
53. Davis R, Anikumar PK, Chandrashekar A, Shamala TR. Biosynthesis of polyhydroxyalkanoates co-polymer in *coli* using genes from *Pseudomonas* and *Bacillus*. Antonie Van Leeuwenhoek. 2008;94:207–216. http://doi.org/10.1007/s10482-008-9233-3.
54. Kihara T, Hiroe A, Ishii-hyakutake M, Mizuno K. *Bacillus cereus* type polyhydroxyalkanoate biosynthetic gene cluster contains R-specific enoyl-CoA hydratase gene. Biosci Biotechnol Biochem. 2017;81:1627-1635. http://doi.org/10.1080/09168451.2017.1325314.
55. Wang X, Li Z, Li X, Qian H, Cai X, Li X, He J. Poly- β -hydroxybutyrate Metabolism Is Unrelated to the Sporulation and Parasporal Crystal Protein Formation in *Bacillus thuringiensis*. Front. Microbiol. 2016;7:1–9.

http://doi.org/10.3389/fmicb.2016.00836.

56. Ho Y, Ju E, Kyum S, Seok Y, Kim J, Dae H, Kim H. Biochemical and Biophysical Research Communications Molecular cloning and characterization of a novel family VIII alkaline esterase from a compost metagenomic library. Biochem Biophys Res Commun. 2010;393:45–49. http://doi.org/10.1016/j.bbrc.2010.01.070.
57. Muchová K, Chromiková Z, Bradshaw N, Wilkinson AJ. Morphogenic Protein RodZ Interacts with Sporulation Specific SpoIIE in *Bacillus subtilis*. Plos one. 2016;11:e0159076. http://doi.org/10.1371/journal.pone.0159076.
58. Dufour A, Haldenwang WG. Interactions between a *Bacillus subtilis* Anti-sigma Factor (RsbW) and Its Antagonist (RsbV). J Bacteriol. 1994;176:1813–1820. http://doi/org/10.1128/jb.176.7.1813-1820.1994.
59. Carniol K, Ben-yehuda S, King N, Losick R. Genetic Dissection of the Sporulation Protein SpoIIE and Its Role in Asymmetric Division in *Bacillus subtilis*. J Bacteriol. 2005;187:3511–3520. http://doi.org/10.1128/JB.187.10.3511.
60. Nakano MM, Zuber P, Glaser P, Danchin A. Two-Component Regulatory Proteins ResD-ResE Are Required for Transcriptional Activation of fnr upon Oxygen Limitation in *Bacillus subtilis*. J Bacteriol. 1996;178:3796–3802. http://doi.org/10.1128/jb.178.13.3796-3802.1996.
61. Walter KA, Nair R V, Caryb JW, Bennettc GN, Papoutsakis ET. Sequence and arrangement of two genes of the butyrate-synthesis of *Clostridium acetobutylicum* ATCC 824. Gene. 1993;134:107–111. https://doi.org/10.1016/0378-1119(93)90182-3.
62. Wei Y, Chen W, Huang C, Wu H, Sun Y. Screening and Evaluation of Polyhydroxybutyrate-Producing Strains from Indigenous Isolate *Cupriavidus taiwanensis* Int J Mol Sci. 2011;12:252–265. http://doi.org/10.3390/ijms12010252.
63. Ye Z, Sangireddy S, Okekeogbu I, Zhou S, Yu C, Hui D, Howe KJ, Fish T, Thannhauser TW. Drought-Induced Leaf Proteome Changes in Switchgrass Seedlings. Int J Mol Sci. 2016;17:1251. http://doi.org/10.3390/ijms17081251.
64. Rangu M, Ye Z, Bhatti S, Zhou S, Yang Y, Fish T, Thannhauser TW. Association of Proteomics Changes with Al-Sensitive Root Zones in Switchgrass. Proteomes. 2018;6:15. http://doi.org/10.3390/proteomes6020015.
65. Yang Y, Qiang X, Owsiany K, Zhang S, Thannhauser TW, Li L. Evaluation of Different Multidimensional LC-MS/MS Pipelines for Isobaric Tags for Relative and Absolute Quantitation (iTRAQ)-Based Proteomic Analysis of Potato Tubers in Response to Cold Storage. J Proeome Res. 2011;10:4647–4660. http://doi.org/10.1021/pr200455s.
66. Chen JW, Scaria J, Mao C, Sobral B, Zhang S, Lawley T, Chang YF. Proteomic Comparison of Historic and Recently Emerged Hypervirulent *Clostridium difficile* J Proteome Res. 2013;12:1151-1161. http://doi.org/10.1021/pr3007528.
67. Yang QS, Wu JH, Li CY, Wei YR, Sheng O, Hu CH, Kuang RB, Huang YH, Peng XX, McCardle JA, Chen W, Yang Y, Rose JK, Zhang S, Yi GJ. Quantitative Proteomic Analysis Reveals that Antioxidation Mechanisms Contribute to Cold Tolerance in Plantain (Musa paradisiaca L.; ABB Group) Seedlings. Mol Cell Proteomics. 2012;11:1853–1869. http://doi.org/10.1074/mcp.M112.022079.
68. Harrington PDB, Vieira NE, Espinoza J, Kae J, Romero R, Yergey AL. Analysis of variance–principal component analysis: A soft tool for proteomic discovery. Analytical Chimica Acta. 2005;544:118–127. http://doi.org/10.1016/j.aca.2005.02.042.
69. Mi H, Muruganujan A, Huang X, Guo X, Thomas PD. Protocol Update for large-scale genome and gene function analysis with the PANTHER. Nature Protocols. 2016;14:703-721. http://doi.org/10.1038/s41596-019-0128-8.
70. Sharma D., Singh R., Deo N, Bishta D. Interactome analysis of Rv0148 to predict potential targets and their pathways linked to aminoglycosides drug resistance: An insilico approach. Microbial Pathogenesis. 2018;121:179-183. https://doi.org/10.1016/j.micpath.2018.05.034.

Table

Table 1 Significantly changed proteins in 24h-12h and 48h-12h samples related with carbohydrate metabolism, stress, sporulation, and energy metabolism.

Function	Accession	Protein description	24h:12h FDR adjusted p-value	Fold Change (24h:12h)	48h:12h FDR adjusted p-value	Fold Change (48h:12h)
Carbohydrate Metabolism	KGT44865	poly(R)-hydroxyalkanoic acid synthase	<.0001	0.75	□	□
	KGT41362	glucose-6-phosphate isomerase	<.0001	0.70	<.0001	0.58
	KGT42918	6-phosphogluconate dehydrogenase	<.0001	0.70	<.0001	0.58
	KGT44986	malate synthase	□	□	<.0001	0.61
	KGT44987	isocitrate lyase	□	□	<.0001	0.66
	KGT41693	phosphate butyryltransferase	□	□	<.0001	1.86
	KGT45740	formate acetyltransferase	□	□	<.0001	2.11
	KGT45741	pyruvate formate lyase-activating protein	□	□	<.0001	2.20
	KGT41354	lactate dehydrogenase	□	□	<.0001	1.81
	KGT44852	amino acid dehydrogenase	□	□	<.0001	1.51
	KGT44853	lactate utilization protein C	□	□	<.0001	1.84
	KGT45530	oxidoreductase	□	□	<.0001	1.50
	KGT44011	ethanol-active dehydrogenase/acetaldehyde-active reductase	□	□	<.0001	1.68
	KGT43462	dihydrolipoamide dehydrogenase	□	□	0.0112	1.72
	KGT43464	pyruvate dehydrogenase	0.0043	1.42	<.0001	1.59
	KGT43465	acetoin:2,6-dichlorophenolindophenol oxidoreductase subunit alpha	<.0001	2.06	<.0001	2.50
	KGT45608	4-aminobutyrate aminotransferase	□	□	<.0001	0.65
	KGT40985	sigma-54 modulation protein	□	□	<.0001	1.54
	KGT44547	acetolactate synthase	□	□	<.0001	0.65
	KGT44564	2-hydroxyacid dehydrogenase	□	□	<.0001	1.52
	KGT45433	butanediol dehydrogenase	□	□	<.0001	1.64
	KGT42393	butanol dehydrogenase	<.0001	0.75	□	□
	KGT42476	dipicolinate synthase subunit A	<.0001	0.68	<.0001	0.57
Stress	KGT43173	glyoxalase	<.0001	0.60	<.0001	0.43
	KGT42737	glyoxalase	<.0001	0.68	<.0001	0.56
	KGT42638	glyoxalase			<.0001	0.64
	KGT44383	glyoxalase	<.0001	0.46	<.0001	0.29
	KGT45443	chemotaxis protein	<.0001	0.76	□	□
	KGT41216	chemotaxis protein	<.0001	0.70	<.0001	0.56
	KGT43768	activator of Hsp90 ATPase 1 family protein	<.0001	0.75	□	□
	KGT44005	molecular chaperone Hsp20	<.0001	2.29	<.0001	2.54
	KGT45779	chaperonin	<.0001	1.35	□	□
	KGT42404	copper resistance protein CopZ	<.0001	1.43	□	□
	KGT42386	RNA-binding protein Hfq	0.0161	1.46	<.0001	1.89
	KGT44525	flagellar hook protein FlgL	□	□	<.0001	1.77
	KGT44484	flagellin	□	□	<.0001	1.61
	KGT45678	molecular chaperone DnaJ	□	□	0.0003	1.86

Function	Accession	Protein description	24h:12h FDR adjusted p-value	Fold Change (24h:12h)	48h:12h FDR adjusted p-value	Fold Change (48h:12h)
	KGT45484	disulfide bond formation protein DsbD	□	□	<.0001	1.74
	KGT42538	anti-terminator HutP	□	□	<.0001	1.52
	KGT41365	general stress protein	□	□	0.0207	1.67
	KGT42051	PhoP family transcriptional regulator	□	□	0.0025	1.58
	KGT43053	stress protein	□	□	<.0001	1.59
Sporulation	KGT40972	cell division protein FtsX	<.0001	0.75	□	□
	KGT41025	peptidase M24	<.0001	0.65	<.0001	0.48
	KGT41076	stage III sporulation protein D	<.0001	0.61	<.0001	0.31
	KGT41078	peptidase M23	<.0001	0.59	<.0001	0.45
	KGT41184	spore gernimation protein GerQ	0.0223	1.42	□	□
	KGT41268	sporulation protein	0.0017	1.66	□	□
	KGT41433	cell division protein FtsQ	<.0001	0.61	<.0001	0.54
	KGT41447	DNA-binding protein	□	□	<.0001	0.48
	KGT41601	sporulation sigma factor SigF	0.0182	1.43	□	□
	KGT41602	anti-sigma F factor	□	□	<.0001	0.65
	KGT41714	stage III sporulation protein AH	<.0001	0.72	<.0001	0.64
	KGT41715	stage III sporulation protein AG	<.0001	1.59	<.0001	1.58
	KGT41946	BofC protein	<.0001	0.66	0.0003	0.54
	KGT41948	spore cortex protein	<.0001	0.69	□	□
	KGT41949	peptigoglycan-binding protein LysM	□	□	<.0001	0.57
	KGT41988	spore coat protein CotS	0.0103	1.49	□	□
	KGT42013	LuxR family transcriptional regulator	<.0001	0.66	<.0001	0.48
	KGT42151	spore protein	0.0247	1.60	□	□
	KGT42445	spore coat protein	<.0001	1.70	□	□
	KGT42520	cell division protein FtsY	□	□	<.0001	1.52
	KGT42664	small acid-soluble spore protein Tlp	<.0001	0.72	□	□
	KGT42674	spore protein P	0.0009	0.62	□	□
	KGT44175	transition state regulator Abh	0.0352	1.75	<.0001	2.75
	KGT44210	Spore coat protein G	<.0001	1.52	□	□
	KGT44211	spore coat protein	<.0001	0.75	0.0012	0.61
	KGT44517	flagellar motor switch protein	<.0001	0.75	□	□
	KGT44707	cell division protein GpsB	□	□	<.0001	2.01
	KGT44778	spore coat protein	□	□	<.0001	0.62
	KGT44827	cell division protein FtsN	<.0001	1.49	□	□
	KGT44878	internalin	<.0001	0.58	<.0001	0.61
	KGT45203	spore protein	0.0067	2.01	0.0189	2.23
	KGT45346	stage V sporulation protein R	□	□	<.0001	0.66
	KGT45552	acid-soluble spore protein H	0.0041	0.70	0.0193	0.50
	KGT45755	spore protein	□	□	0.0025	0.45
	KGT45877	sporulation protein	<.0001	0.76	<.0001	0.54

Function	Accession	Protein description	24h:12h FDR adjusted p-value	Fold Change (24h:12h)	48h:12h FDR adjusted p-value	Fold Change (48h:12h)
	KGT45955	spore gernimation protein GerD	<.0001	0.64	<.0001	0.47
	KGT45975	protein sspF	<.0001	1.90	0.0014	1.52
	KGT45993	stage II sporulation protein E	0.0233	1.50	□	□
Energy Metabolism	KGT41105	ATP F0F1 synthase subunit B	<.0001	0.67	<.0001	0.60
	KGT45463	quinol oxidase subunit 2	□	□	<.0001	1.57
	KGT44670	menaquinol-cytochrome C reductase	0.0042	1.35	<.0001	1.77
	KGT42309	cytochrome D ubiquinol oxidase subunit I	□	□	<.0001	2.33
	KGT44113	nitrate reductase	□	□	<.0001	2.47
	KGT44114	nitrate reductase	□	□	<.0001	1.92
	KGT44115	nitrate reductase	□	□	<.0001	2.75
	KGT44130	nitrite reductase	0.0004	1.92	<.0001	2.65
	KGT44131	nitrite reductase	□	□	<.0001	2.48

Accession: Protein accession from NCBI database; Protein description: Protein NCBI description; Fold change (24h:12h) and (48h:12h) were obtained from anti-log conversion of $\log_2$ ratios.

Figures

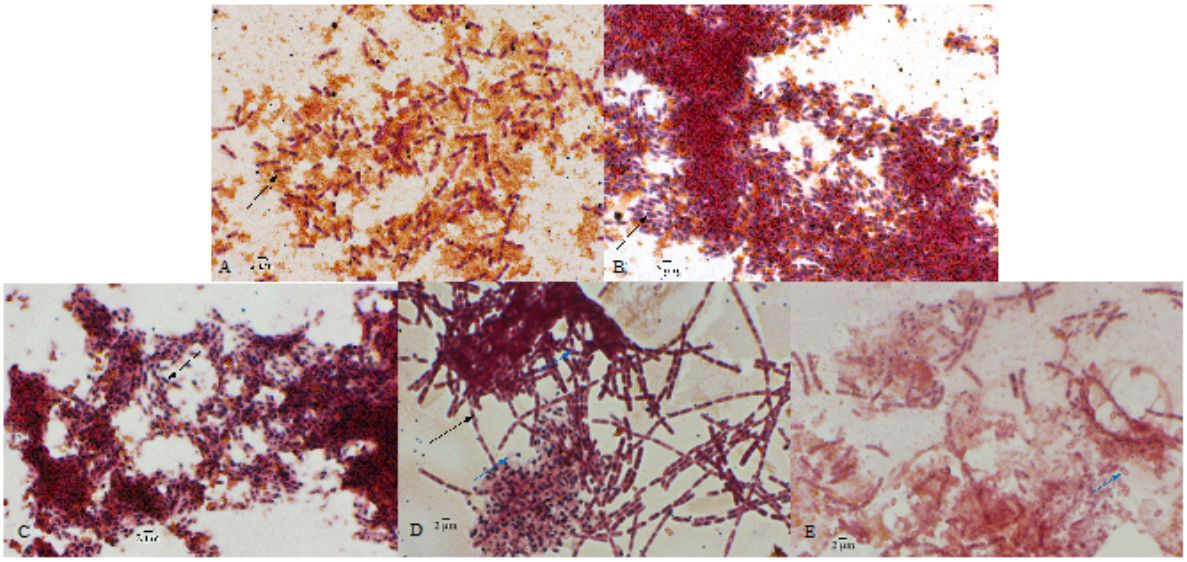

Figure 1

PHB accumulation status in B. cereus tsu1. B. cereus tsu1 was cultured in RCS medium for 6 h (A), 9 h (B) and 12 h (C), 24 h (D), 48 h (E). In RCS medium, PHB accumulation was observed at an early stage (6 h) and reached highest accumulation before 12 h. Fore-spore and spore structure was observed at 24 h, significant PHB degradation was observed at 48 h. (Black arrow indicates PHB; blue arrow indicates fore-spore and spore).

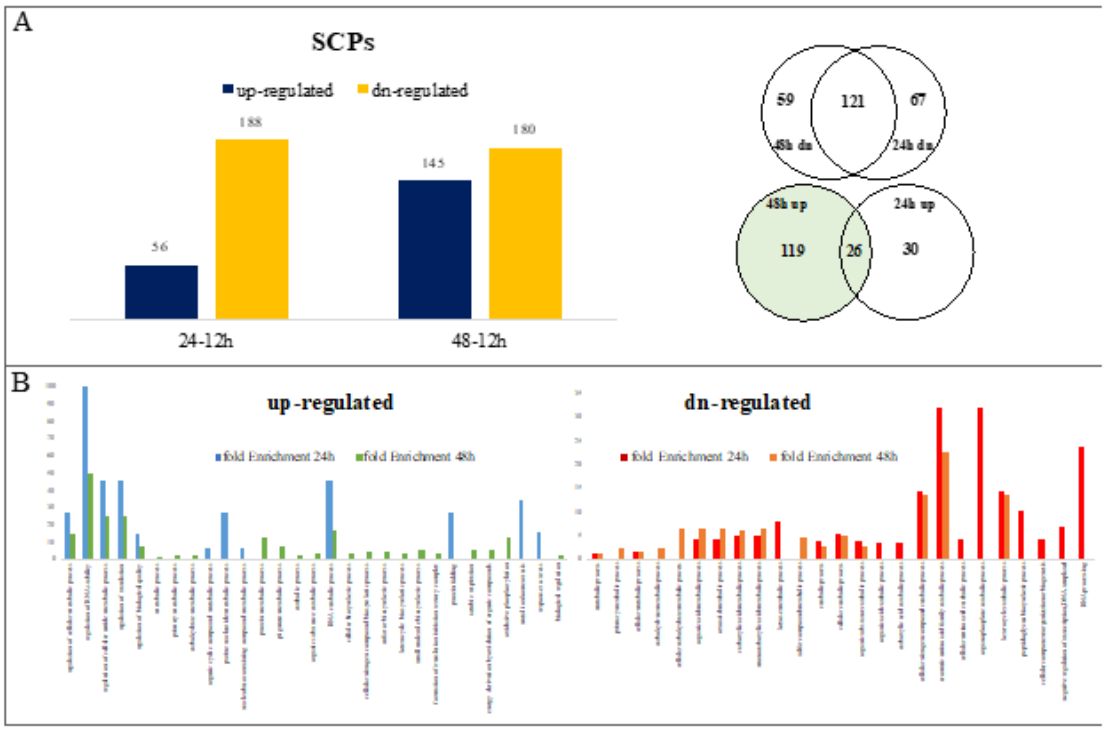

Figure 2

Significantly changed proteins (SCPs), and gene ontology classification using the PANTHER classification system. A: SCPs were compared between 24h- and 12h-cultures (56 up-regulated proteins, 188 down-regulated protein), between 48h- and 12h-cultures (145 up-regulated, 180 down-regulated); Venn diagram shows common and unique SCPs in 24h-12h and 48h-12h samples. B: Gene ontology classification. The enriched biological processes in 24 up-regulated SCPs (blue), 48 up-regulated SCPs (green), and 24 down-regulated SCPs (red), 48 down-regulated SCPs (orange) were compared. Proteins assigned to at least one category could be counted more than once.

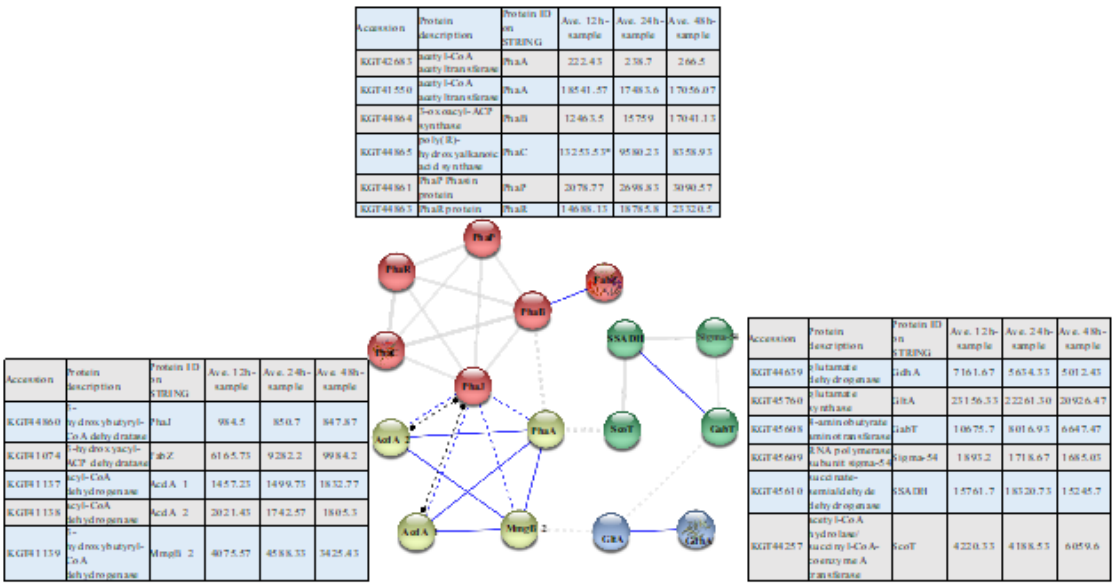

Figure 3

STRING protein interaction network of enzymes for PHB biosynthesis pathways, and protein abundance levels over time. STRING version 10.5 was used to construct protein–protein interaction networks of PHB biosynthesis enzymes in annotated genome of B. cereus tsu1. Medium confidence (0.400) was applied and disconnected nodes were hidden. MCL clustering was using inflation parameter 3. Lines between nodes represent their action effects. Enzymes for PHB biosynthesis and their abundance level at three time points are listed in Additional file 1: Table S1-6.

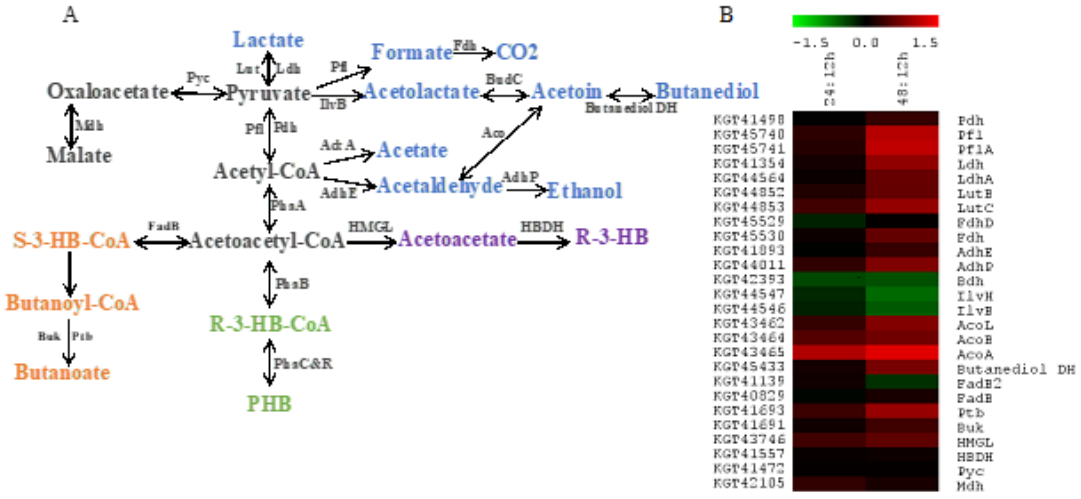

Figure 4

Schematics of pathways related with PHB intracellular mobilization in B. cereus tsu1. A: Interactions between PHB intracellular mobilization, and other major related pathways. Glycolysis, lipid and amino acid metabolism, and TCA provide carbon resource for PHB biosynthesis. Pyruvate (anaerobic) fermentation, butanoate metabolism compete carbon resource with PHB synthesis. Enzymes and their abundance level at three time points are listed in Additional file 1: Table S1-3. B: Heat map shows log2 transformed fold changes of proteins in pathways related with PHB intracellular mobilization.

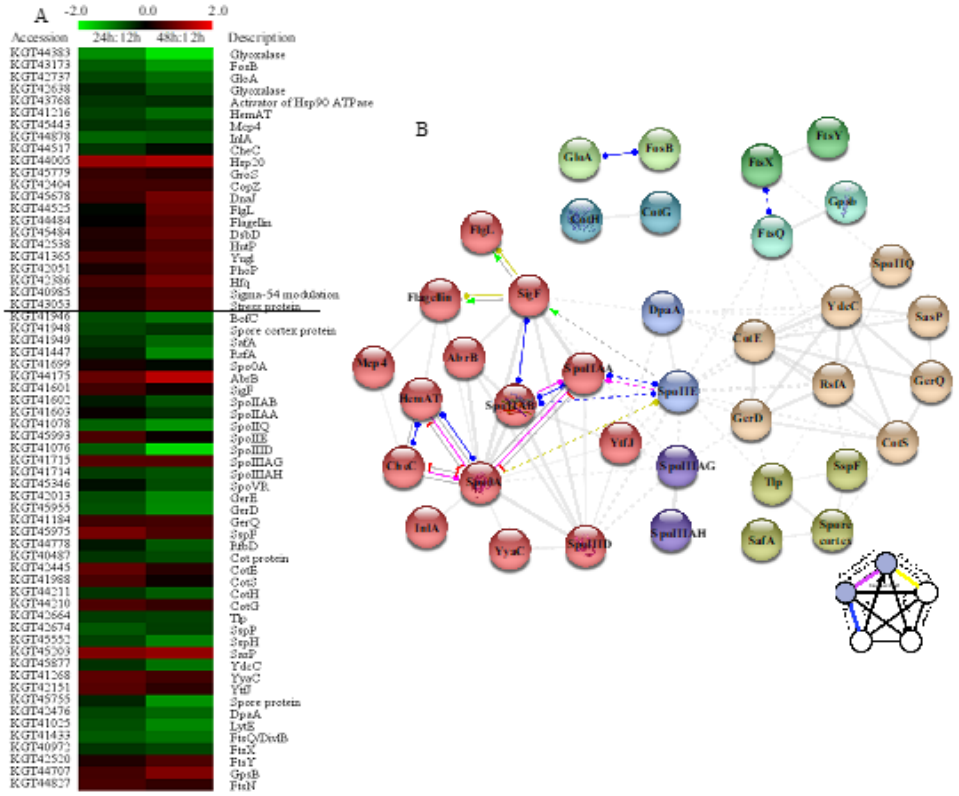

Figure 5

Sporulation-related and stress-induced proteins. A: Heat map displays log2 fold changes of proteins associated with stress and sporulation annotated on B. cereus tsu1. B: STRING version 10.5 was used to build protein–protein interaction networks of significantly changed sporulation and stress proteins. The lines in between two nodes indicate the predicted mode of actions. Red nodes represent proteins regulating sporulation process. Gene spoII E is an activator of sigF, which is a regulator of asymmetric division and flagella proteins.

Supplementary Files

This is a list of supplementary files associated with this preprint. Click to download.

- AdditionalFile1.xlsx
- AdditionalFile4.docx
- AdditionalFile3.xlsx
- AdditionalFile2.xlsx